

Thin Film Electrode of Prussian Blue Analogue for Li-ion Battery

Yutaka Moritomo^{1,2,3}, Masamitsu Takachi², Yutaro Kurihara³, and Tomoyuki Matsuda³

¹TIMS, University of Tsukuba, Tsukuba305-8571, Japan

²School of Science and Engineering, University of Tsukuba, Tsukuba, Ibaraki 305-8571, Japan

³Graduated School of Pure and Applied Science, University of Tsukuba, Tsukuba 305-8571, Japan

1 Introduction

Next-generation electrode materials that provide rapid and reversible Li⁺ insertion/extraction have been intensively explored in order to achieve a low-cost Li⁺ secondary battery (LIB) with a high charge/discharge rate. Recently, Matsuda and Moritomo[1] reported that a thin film of the Prussian blue analogue, Na_{1.32}Mn[Fe(CN)₆]_{0.83}3.5H₂O exhibits a large capacity (= 128 mAh/g) and good cyclability (= 87% of the initial value at 100 cycles).

In this study, we investigated the Li⁺ intercalation speed in thin film electrodes of the Prussian blue analogues (Li,Na)_{4y-2}M[Fe(CN)₆]_yzH₂O (M = Ni, Co, Mn and Cd). X-ray powder diffraction (XRD) measurements revealed that the Li-substituted compounds are face-centered cubic (Fm $\bar{3}$ m; Z = 4). The X-ray absorption fine structure (XAFS) near the Fe K-edge revealed the reduction of Fe (Fe³⁺ → Fe²⁺) with the Li⁺ intercalation. The reduction of Fe causes a significant color change of the thin film electrodes.

2 Experiment

Thin films of Na_{0.72}Ni[Fe(CN)₆]_{0.68}5.1H₂O (denoted as NNF68), Na_{0.84}Co[Fe(CN)₆]_{0.71}3.8H₂O (NCF71), Na_{1.24}Mn[Fe(CN)₆]_{0.81}3.0H₂O (NMF81), and Na_{1.84}Cd[Fe(CN)₆]_{0.96}4.8H₂O (NCdF96) were electrochemically synthesized on an indium tin oxide (ITO) transparent electrode under potentiostatic conditions at - 0.50 V vs a Ag/AgCl electrode in an aqueous solution. The thicknesses of the films were 1 μm, which were measured with a profilometer (Dektak3030). The mass of each film was measured with a conventional electronic weighing machine after the film was carefully removed from the ITO glass with a microspatula. The experimental error of the mass is 10%. Chemical compositions of the films were determined by the inductively coupled plasma (ICP) method and CHN organic elementary analysis (Perkin-Elmer 2400 CHN Elemental Analyzer). Rietveld analysis of the XRD pattern revealed that the compounds are face-centered cubic with lattice constant a = 10.200(3) Å for NNF68, 10.296(2) Å for NCF71, 10.544(2) Å for NMF81, and 10.7001(4) Å for NCdF96. The Li⁺ was substituted for Na⁺ by performing charge/discharge cycles of the thin films against Li. The electrolyte was ethylene carbonate (EC)/diethyl carbonate (DEC) solution containing 1 mol/L LiClO₄. The charge/discharge current is 10 μA (= 0.5 - 1.0 C), and the cutoff voltage was from 2.0 to 4.2 V.

Thus, we obtained thin film electrodes, i.e., Li_xNa_{0.04}Ni[Fe(CN)₆]_{0.68}5.1H₂O (M = Ni), Li_xNa_{0.13}Co[Fe(CN)₆]_{0.71}3.8H₂O (M = Co), Li_xMn[Fe(CN)₆]_{0.81}3.0H₂O (M = Mn), and Li_xNa_{0.88}Cd[Fe(CN)₆]_{0.96}4.8H₂O (M = Cd). In the XRD and XAFS experiments, the Li concentration (x) was controlled by the cutoff voltage.

The valence states of the Fe, Mn, Ni, Co, and Cd sites were determined by the *ex-situ* X-ray absorption spectra (XAS) around the K-edge and L₁-edge spectra. The XAS measurements were conducted at the beamline 7C of the Photon Factory, KEK. The XAS spectra were recorded by a Lytle detector in a fluorescent yield mode with a Si(111) double-crystal monochromator at 300 K. The background subtraction and normalization were done using ATHENA program[2].

The *ex-situ* powder X-ray diffraction (XRD) patterns were measured at the beamline 8A of KEK-PF equipped with an imaging plate detector. The charged/discharged samples were washed with DEC, and were carefully removed from the ITO glasses. The obtained powders were sealed in 300 μm glass capillaries. XRD patterns were measured at 300 K and the exposure time was 10 min. Wavelength of the X-ray was 0.77474 Å. The lattice constants of each compounds were refined by the RIETAN-FP program [3].

3 Results and Discussion

Figure 1 shows the XAFS spectra of the thin film electrodes against x. The measurements were carried out at the 7C beamline of Photon Factory (PF), KEK. The XAFS spectra near the Fe K-edge, Ni K-edge, Co K-edge, Mn K-edge, and Cd L₁-edge were recorded by a Lytle detector in fluorescent yield mode with a Si(111) double-crystal monochromator and were normalized by the intensities at 7140, 8360, 7740, 6560, and 4060 eV, respectively. In all the compounds, the absorption peaks in the Fe K-edge spectra [Figs. 2(a), 2(c), 2(e) and 2(g)] show a redshift with increasing in x. The redshift is ascribed to the reduction of Fe (low-spin Fe³⁺ → low-spin Fe²⁺). The reduction of Fe causes a significant color change, as shown in Fig.2, which can be utilized as a battery power monitor. On the other hand, the absorption peaks in the Ni K-edge [(b)], Co K-edge [(d)], Mn K-edge [(f)], and Cd L₁-edge [(h)] spectra show no shift, indicating that the valence states of M remain unchanged.

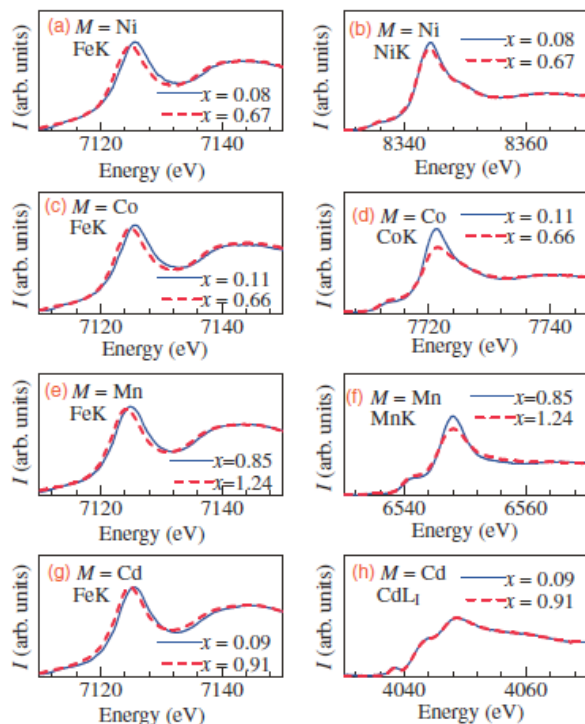


Fig. 1: X-ray absorption spectra of $\text{Li}_x\text{Na}_{0.04}\text{Ni}[\text{Fe}(\text{CN})_6]_{0.68}5.1\text{H}_2\text{O}$ [(a) and (b)], $\text{Li}_x\text{Na}_{0.13}\text{Co}[\text{Fe}(\text{CN})_6]_{0.71}3.8\text{H}_2\text{O}$ (c) and (d)], $\text{Li}_x\text{Mn}[\text{Fe}(\text{CN})_6]_{0.81}3.0\text{H}_2\text{O}$ [(e) and (f)], and $\text{Li}_x\text{Na}_{0.88}\text{Cd}[\text{Fe}(\text{CN})_6]_{0.96}4.8\text{H}_2\text{O}$ [(g) and (h)] against x . The two spectra completely overlap each other in (h)

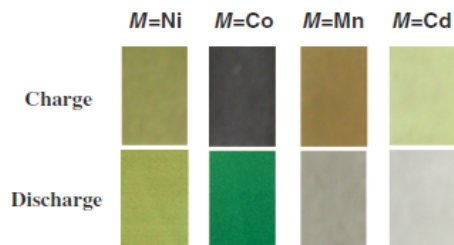


Fig. 2: Color of thin-film electrodes of the Prussian blue analogues, $\text{Li}_x\text{Na}_{0.04}\text{Ni}[\text{Fe}(\text{CN})_6]_{0.68}5.1\text{H}_2\text{O}$ ($M = \text{Ni}$), $\text{Li}_x\text{Na}_{0.13}\text{Co}[\text{Fe}(\text{CN})_6]_{0.71}3.8\text{H}_2\text{O}$ ($M = \text{Co}$), $\text{Li}_x\text{Mn}[\text{Fe}(\text{CN})_6]_{0.81}3.0\text{H}_2\text{O}$ ($M = \text{Mn}$), and $\text{Li}_x\text{Na}_{0.88}\text{Cd}[\text{Fe}(\text{CN})_6]_{0.96}4.8\text{H}_2\text{O}$ ($M = \text{Cd}$), in the charge and discharge states

Figure 3 shows examples of the XRD patterns of $\text{Li}_x\text{Na}_{0.13}\text{Co}[\text{Fe}(\text{CN})_6]_{0.71}3.8\text{H}_2\text{O}$. We confirmed that the XRD patterns of all the compounds can be indexed with the face-centered cubic ($\text{Fm}\bar{3}\text{m}$; $Z = 4$) setting, as shown in Fig. 3. The lattice constants (a) are plotted in Fig. 4 against x . Except for the Cd compound, a slightly decreases with increasing in x . The decrease in a is probably due to the smaller size of $[\text{Fe}^{\text{II}}(\text{CN})_6]^{4-}$ than that of $[\text{Fe}^{\text{III}}(\text{CN})_6]^{3-}$. Actually, the $\text{Fe}^{\text{II}} - \text{N}$ bond length ($= 3.00 - 3.01 \text{ \AA}$) is shorter than the $\text{Fe}^{\text{III}} - \text{N}$ bond length ($= 3.10 \text{ \AA}$) in $\text{RbMn}[\text{Fe}(\text{CN})_6]$. In the Mn compound, a decreases in the Mn redox region ($x < 0.24$).

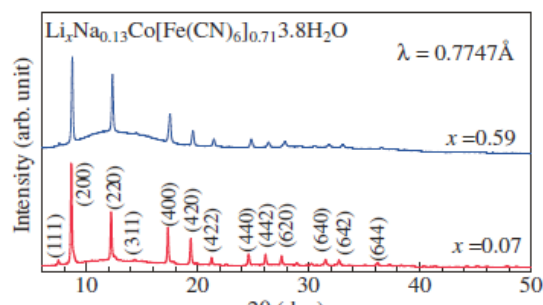


Fig. 3: X-ray diffraction patterns of $\text{Li}_x\text{Na}_{0.13}\text{Co}[\text{Fe}(\text{CN})_6]_{0.71}3.8\text{H}_2\text{O}$ against x . Parentheses represent indexes in the face-centered cubic setting.

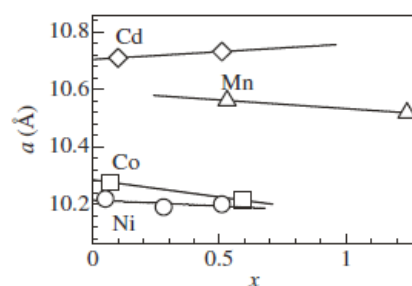


Fig. 4: Lattice constant (a) of $\text{Li}_x\text{Na}_{0.04}\text{Ni}[\text{Fe}(\text{CN})_6]_{0.68}5.1\text{H}_2\text{O}$ (circles), $\text{Li}_x\text{Na}_{0.13}\text{Co}[\text{Fe}(\text{CN})_6]_{0.71}3.8\text{H}_2\text{O}$ (squares), $\text{Li}_x\text{Mn}[\text{Fe}(\text{CN})_6]_{0.81}3.0\text{H}_2\text{O}$ (triangles), and $\text{Li}_x\text{Na}_{0.88}\text{Cd}[\text{Fe}(\text{CN})_6]_{0.96}4.8\text{H}_2\text{O}$ (diamonds) against x . Straight lines are results of the least-squares fitting, and also represent the Fe redox region

Acknowledgement

This work was supported by a Grant-in-Aid (21244052) for Scientific Research from the Ministry of Education, Culture, Sports, Science and Technology. Elementary analysis was performed at Chemical Analysis Division, Research Facility Center for Science and Engineering, University of Tsukuba. The X-ray powder diffraction and X-ray absorption experiments were performed under the approval of the Photon Factory Program Advisory Committee (Proposal No. 2010G502 and 2011G501).

References

- [1] T. Matsuda, and Y. Moritomo, Appl. Phys. Express, **4** (2012) 047101.
- [2] B. Ravel, and M. Newville, J. Synchrotron Radiation, **12** (2005) 537-541.
- [3] F. Izumi, and K. Momma, Solid State Phenomena, **130** (2007) 15-20.

* pf-acr2011@kek.jp